Power Losses Measurement Method for High Efficiency MV Oil-Insulated DC-DC Converter

Pierre Le Métayer, Cyril Buttay, Piotr Dworakowski, Drazen Dujic

Power Losses Measurement Method for High Efficiency MV Oil-Insulated DC-DC Converter

Pierre Le Métayer[1], Cyril Buttay[2], Piotr Dworakowski[1], Drazen Dujic[3]

[1] SuperGrid Institute, France

[2] Univ Lyon, CNRS, INSA Lyon, Université Claude Bernard Lyon 1, Ecole Centrale de Lyon, Ampère, UMR 5005, France

[3] Ecole Polytechnique Fédérale de Lausanne (EPFL), Power Electronics Laboratory, Switzerland

Corresponding author: Pierre Le Métayer, pierre.lemetayer@supergrid-institute.com

Speaker: Pierre Le Métayer, pierre.lemetayer@supergrid-institute.com

Abstract

The concept of MVDC collection network for renewable applications requires a high efficiency DC-DC converter to connect low voltage sources to the medium voltage network. The accurate measurement of low power losses is not possible with traditional electrical input-output power measurements. This paper adopts and extends a transient calorimetric method suited for the measurement on such converters. It is shown experimentally that this method can be applied to the measurement of the losses of an oil-immersed DC-DC converter. The maximum efficiency of the 83 kW, 1.2 to 6.6 kV prototype is measured at 99.16 ±0.04% (99.12…99.20%).

1 Introduction

The concept of MVDC power collection in renewable energy plants has seen increasing interest in both academic [1]–[3] and industrial environments [4]. A critical piece to connect the low voltage sources to the MVDC power collection network is the LV-to-MV DC-DC converter [5]–[7]. The converter proposed in [6] has four elements experiencing medium voltage: the medium frequency transformer (MFT), the rectifier, the filter inductor and the filter capacitor. The large insulation distances required in air between all the components of the MV circuit may result in a bulky converter. As presented in [8], we proposed to immerse all the components of the MV circuit in a dielectric fluid, both for electrical isolation and thermal management purposes. An illustration of the complete DC-DC converter mechanical design and its schematic are shown in Fig.1.

The efficiency of the DC-DC converter has been identified as the key criterion for the development of MVDC in photovoltaic production [3]. The accurate measurement of losses is thus paramount when one wants to verify the performance of such a high efficiency converter (efficiency ~99%).

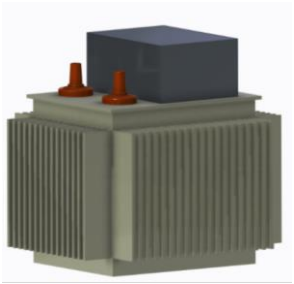

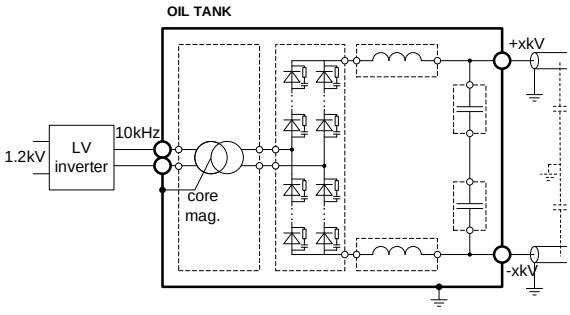

Fig. 1 Top: LV to MV DC-DC implementation with the LV inverter represented as the grey box sitting on top of the oil tank containing all the medium voltage elements (MFT, rectifier, output filter); bottom: Schematic of the medium voltage unidirectional DC-DC converter (Phase Shift Full-Bridge (PSFB) topology).

It was shown in [9] that simple electrical input-output measurement (the so-called “indirect method”) of a high efficiency MV converter would be too uncertain. Indeed, the uncertainty associated with the electrical measurement of the 99% efficiency of a 25 kW, 7 kV inverter (based on 10 kV SiC MOSFETs) was found as ±0.83 percentage points (98.17…99.83%), which makes the measurement untrustable. Because of the uncertainties on the measurement of high power, the accuracy of indirect methods is of the same order of magnitude as the power losses themselves. Therefore, losses must be measured using a direct method.

This paper first presents the different methods existing in the literature for the direct measurement of power losses and selects one suited for the particular case of a high-ratio, unidirectional converter. This method is described in the second section. The contribution of this paper is the extension of the selected method to the measurement of the losses in the oil tank. This is demonstrated experimentally, first on a small-scale prototype and then on a full-scale medium voltage DC-DC converter tank (the inverter losses measurement is not presented in this paper). Finally, a discussion on the pros and cons of this method is made.

2 Direct losses measurement methods

A set-up like the one shown at the top of Fig. 2, can be implemented to electrically measure the losses directly. In this scheme, the DC power supply only provides the power losses of the circuit, while the rated power only flows in the closed loop. Here, the measurement of the power supplied is accurate since the losses are measured directly, and not as the small difference between two large quantities [10]. However, losses of the complete circuit are measured, including the cables.

Alas, this method is only applicable for converters with a voltage ratio of 1:1, since the output is connected to the input. This limitation can be overcome by using the “back-to-back” or opposition method [11] scheme presented in Fig. 2, with one converter of ratio 1:r and the other of ratio r:1. In this case, the supplied power corresponds the power losses of both converters. The repartition between the two converters is known only in the case of identical, bidirectional converters. Indeed, bidirectional converters can be structurally symmetrical, with the same components on their respective low voltage and medium voltage sides.

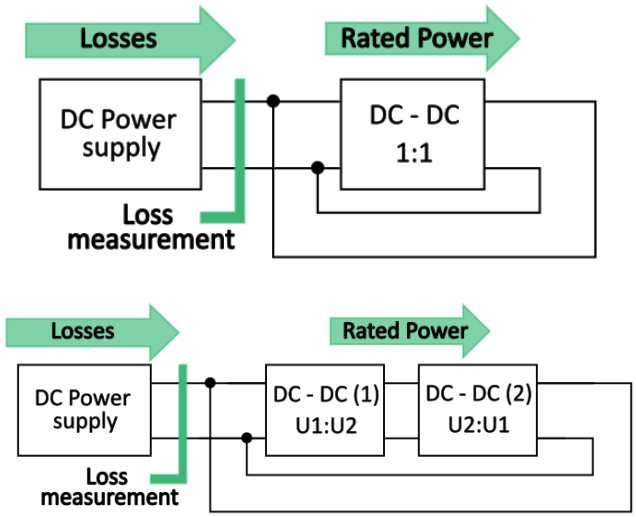

Fig. 2 Circuits for direct electrical measurement of the power losses (top: “standalone”; bottom: “back-to-back” or opposition method)

However, with unidirectional converters (as is the case with the PSFB studied here), the 1:r and r:1 converters would be different. One could not ensure they have identical losses, and it is no longer possible to separate the losses of each converter from the measurement of the total losses.

Since the electrical methods are either not accurate enough or not implementable for a unidirectional step-up converter, one must resort to calorimetric methods. The different categories of calorimetric methods are summarised in Fig. 3.

In flow calorimetry, a fluid is used to collect the heat generated by the power losses. The power losses can be estimated knowing the specific heat capacity c_p of the fluid, by measuring the temperature difference between inlet and outlet (ΔT) and the mass flow-rate $\dot{m}$ of the cooling fluid at equilibrium [12].

$$P_{loss} = c_p \, \Delta T \, \dot{m} \tag{1}$$

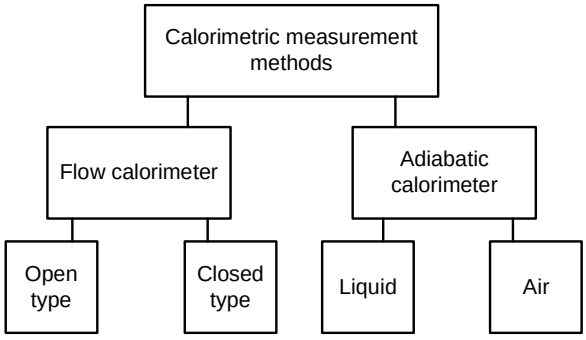

Fig. 3 Calorimetric measurement methods categories

In open type calorimeters, the cooling fluid is air as the device under test is directly put in the measurement circuit. In closed type, a different fluid can be selected, such as water, as the measurement circuit uses a heat exchanger in contact with the device under test. This second type is generally more accurate as the cooling fluid is less sensitive to environmental conditions than air. In our case, the converter prototype is passively air-cooled. The implementation of a flow calorimeter would require an additional cooling circuit. This makes this method difficult to apply, as it changes the general operation of the converter.

An adiabatic calorimeter does not require any flow-rate measurement, as it does not have any heat exchange with the environment. The power losses are then calculated as [13]:

$$P_{loss} = \Delta T \, C_{th} \, / \, t \qquad (2)$$

with C_{th} the total heat capacity inside of the adiabatic enclosure (typically filled with a liquid to collect and distribute the heat generated by the converter) and t the duration of the test during which the liquid temperature has increased by ΔT. It is pointed out in [13] that equation (2) is true only for constant power dissipation over time, uniform temperature in the calorimeter, and constant heat capacity. Measurements are performed in a transient state, as the enclosure heats up continuously; therefore, ΔT must be kept small, to ensure there is no change in the converter's operating point, and to keep test duration short in the case of large converters. In our case, given the size of the converter, adiabatic calorimeters would be unpractical

Because of the limitations of the calorimetric measurement methods displayed in Fig. 3, the authors of [14] propose a hybrid method . It uses an open flow calorimeter (in the sense that heat is exchanged with the surrounding air), but has a transient operation, much like an adiabatic calorimeter: this method is based on measuring the time-derivative of the temperature difference with the ambient air (ΔT), referred to as the slew rate (SR) in this document. In [14] the method is applied to estimating the losses of power modules in an automotive inverter.

3 In-air transient calorimetric method

3.1 Description of the method

Loss measurement using the in-air transient calorimetric method is divided into two stages: a first calibration stage, followed by a measurement stage. The Fig. 4 shows a diagram explaining the main steps of the method.

For the calibration stage, temperature elevation data during the thermal transient response is monitored for different, known values of DC power injected in the system under test. The temperature data is then processed (filtering out measurement noise) and the temperature SR is calculated over the same temperature range for each operating point. These SR values are processed and plotted on an SR vs Power injected graph. The resulting point cloud is used to fit a calibration curve, which establishes a relationship between SR and electrical losses. One calibration curve is specific to an object and a test environment. The calibration step must therefore be repeated for any change in configuration or ambient thermal conditions (air flow, temperature sensor position).

The measurement operation comes in a second stage, under the same thermal conditions as the calibration phase. During this stage, the transient temperature variation is monitored when the converter is operated under a given load, with unknown power losses. Following similar data processing steps as in the calibration stage, a SR value is calculated. Finally, the corresponding loss value is deduced by reading the calibration graph.

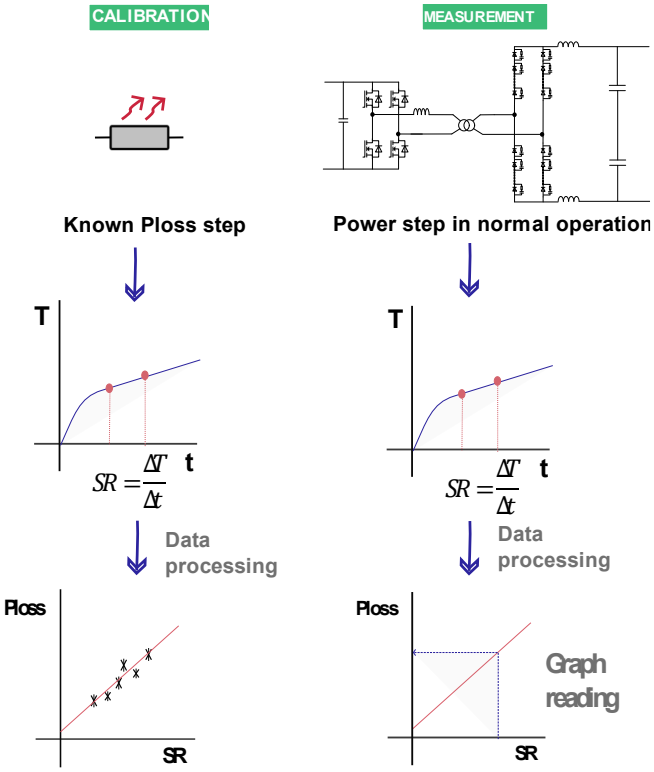

Fig. 4 Steps of the selected calorimetric method

The relative uncertainties associated with the power losses measurement using this method are estimated to be less than 5% in [14], with the temperatures measured using Negative Temperature Coefficient (NTC) resistor. This is considered very satisfactory compared to the other method that does not require changing the converter environment (the "input-output" electrical method).

3.2 Small-scale experimental validation

The validation of the in-air transient calorimetric method on an oil-immersed converter is particularly important, as the original paper [14] focuses on power module in an in-air inverter, an object quite remote from our test case. To that effect, a test bench with a small-scale model is set up. It consists of a cut-out jerrycan filled with Midel 7131 oil, into which resistors are immersed. A Plexiglas plate is placed on the upper part of the tank to limit convective exchanges with the ambient air. The configuration of the test bench (Fig. 5) is adapted to investigate the following items: location of the temperature probe and representativity of the calibration resistor.

The oil in the tank is in contact with all the components, so it collects all the heat they generate. Measuring the oil temperature should therefore give a perfect image of the losses. Unfortunately, the oil temperature is not uniform in the tank, as natural convection occurs in the oil. Furthermore, there is no certainty that the oil flows caused by natural convection remain identical when the distribution of the losses changes between the components. Evaluating these sources of uncertainty is the objective of the test described here.

Regarding the location of the temperature probes, a first probe is placed on the outer wall of the oil tank, and a second probe is placed inside the tank, immersed in the oil. Indeed, the oil tank gives the opportunity to measure the temperature of a liquid containing all of the power loss sources, similarly as in the adiabatic calorimeter method. The measurement on the tank wall is closer to the method described in [14]. Another temperature probe is also placed in the ambient air to calculate the relative temperature increase. The set-up is shown in Fig. 5. The thermal camera picture shows that the temperature of the tank wall is constant for a certain horizontal level. A gradient is observed from high temperatures at the top to lower temperatures at the bottom.

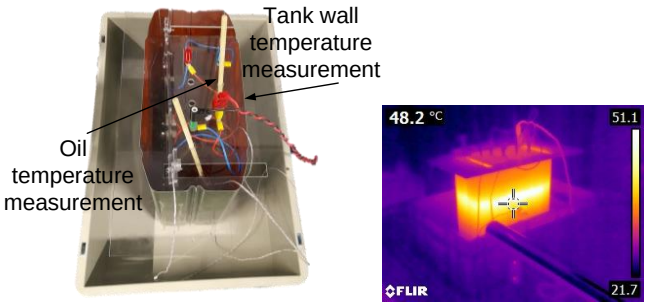

Fig. 5 Left: Jerrican filled with oil (Midel 7131) used as small-scale test set-up for the oil tank; right: thermal camera picture of the oil tank showing that tank wall is hottest at the top oil level.

To assess the effect of the distribution of the heat sources in the tank, first a calibration campaign is carried out using a flat rectangular resistor (Stego HV 031, 132 Ω) immersed in the tank of the small-scale model. Known power steps are injected into the calibration resistor and the temperature rises in the oil and on the tank are measured. The corresponding SR are calculated.

In a validation stage, a second, identical, resistor is added. The aim is to emulate a different location and distribution of losses in the tank, as would be the case with the actual tank components (MFT, rectifier, inductors). A resistor with a cylindrical ceramic heatsink is also selected to observe the influence of thermal properties on the temperature rise measurements. Tests are carried out by injecting power into this resistor placed vertically and then horizontally in the tank, to study the influence of convection conditions in the tank on the various measurements. The different set-ups are summarised in Fig. 6. The temperature ranges over which the SR is calculated are 35-45°C for the tank wall and 45-55°C for the oil measurement. The results of the calibration and validation stages are shown on Fig. 7.

The maximum relative error between the calibration points and the calibration curves are 11% for the oil measurement and 5.2% for the outer wall.

Measurements performed on the outer wall of the tank result in a more linear distribution of losses as a function of temperature rise. The calibration point at 420 W is performed twice at a different ambient temperature (24°C, 28°C). This second point also allows us to note that the measurement on the outer wall of the tank is more robust to ambient temperature variation than the measurement in the oil.

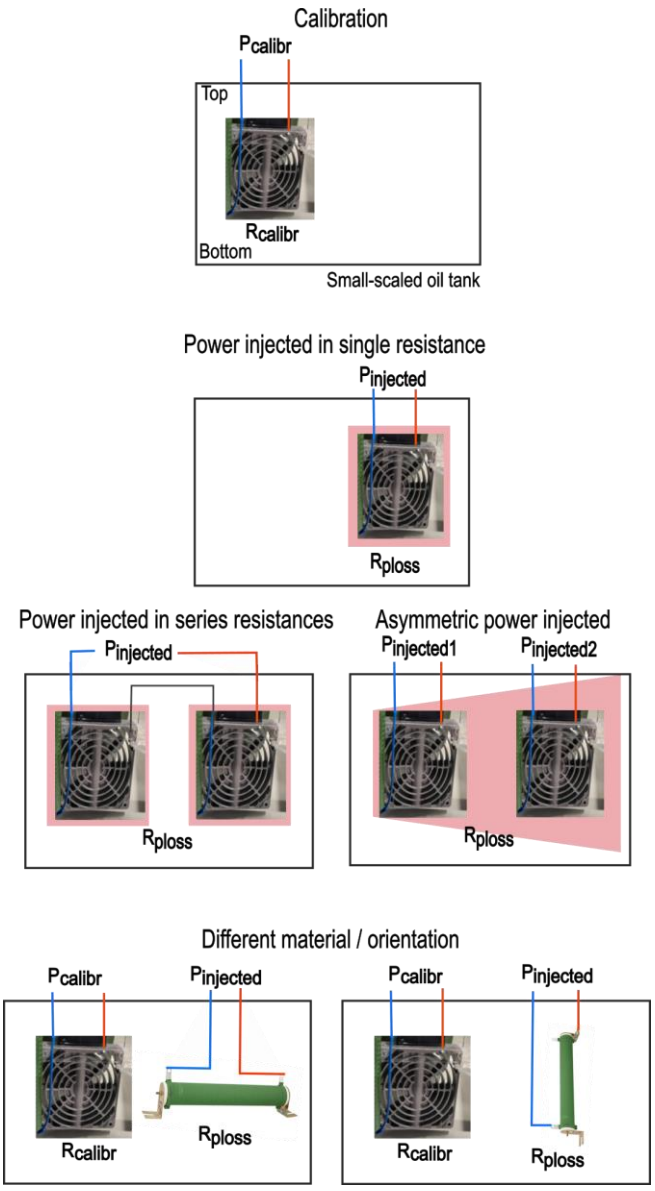

Fig. 6 Summary of the different test set-up configurations

The maximum relative error between the validation points and the calibration curves is 40% for the oil measurement and 9% for the tank outer wall measurement. For both the temperature measurements the biggest relative errors between the electrical measurement and the respective calibration curve occur for the setup with the ceramic resistor positioned horizontally in the tank.

One could have predicted that the oil measurement method would lead to worst results as it was stated that the adiabatic liquid calorimeter method relies on a uniform temperature in the calorimeter. This is absolutely not the case here since no stirring is performed, contrarily to in [13].

It can be deduced from these tests that the temperature measurement on the outer wall of the tank is more robust to variations in the geometry or technology of the loss source. Heat conduction in the metallic wall of the tank probably produces an averaging phenomenon, which makes the measurement on the outer wall of the tank more robust to changes in the convection conditions and the proprieties of the heat source. With a maximum relative error of 9%, this measurement method is considered satisfactory (compared to the high uncertainties of electrical methods).

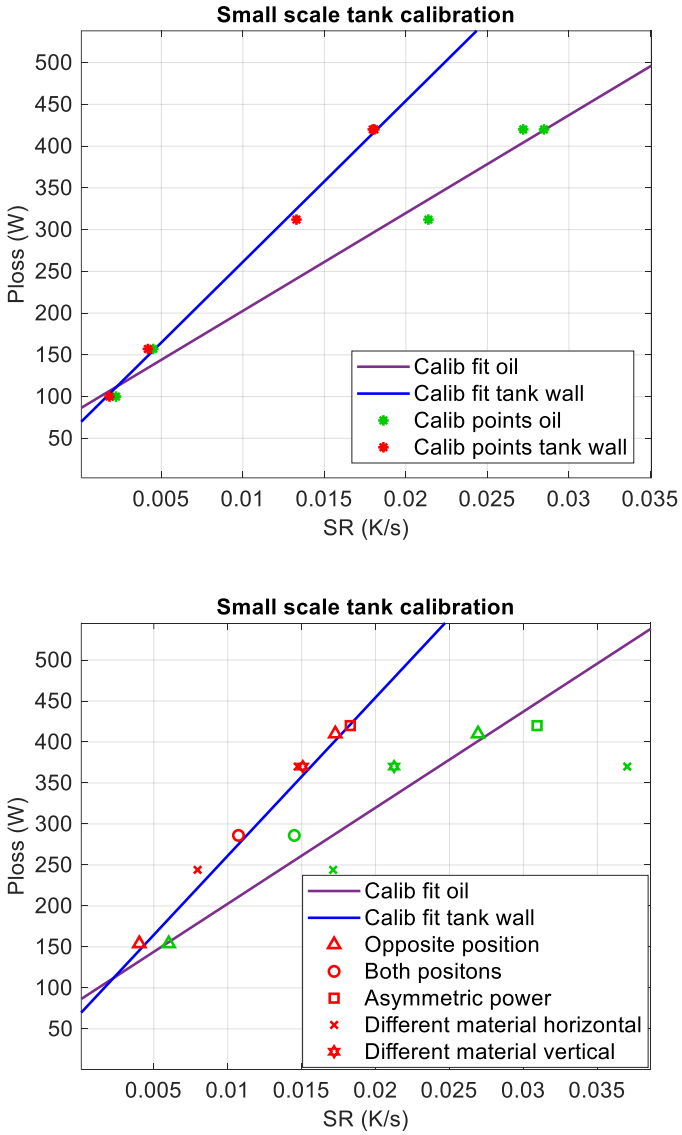

Fig. 7 Top: Calibration points and resulting fitted curves for the measurement in oil (green and purple) and on the tank wall (red and blue); bottom: Comparison of the measured values for different locations of the heat-dissipating elements in the tank and the calibration curves

4 DC-DC converter power losses measurement

The previously described and validated method is applied to the full-scale prototype of oil-immersed DC-DC converter presented in Fig. 8 and described in details in [15], in order to measure its efficiency. Resistors (4, 132 Ω Stego HV 031) are placed in the tank for the calibration step together with the other elements and supplied with DC power using feedthrough connectors.

The temperature transient curves, with their associated SR calculation zones (black lines), and resulting calibration curves are shown in Fig. 9. One can appreciate the advantage of the transient calorimetric method by looking at the duration of the tests. Indeed, with the selected SR calculation zones, the tank test duration is kept below 2 hours. This is especially important for the tank as its thermal steady state would be reached after more than a day (the estimated thermal time constant of the tank is 4.9 hours). The formulas used for uncertainty calculations can be found in Appendix.

The converter prototype is operated at different power loads thanks to a back-to-back configuration (as in Fig. 2), with the second converter being a Buck converter based on series connection of MOSFETs as presented in [16]. Power steps are applied, and the temperature on the tank wall is measured to deduce the power losses.

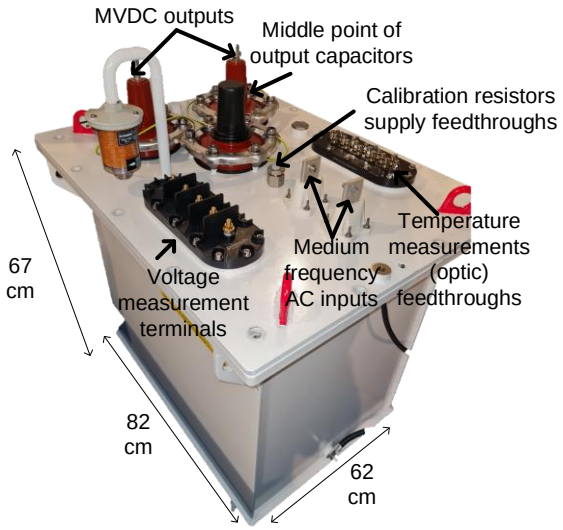

Fig. 8 Oil tank of the full-scale 83 kW 1.2-6.6 kV prototype

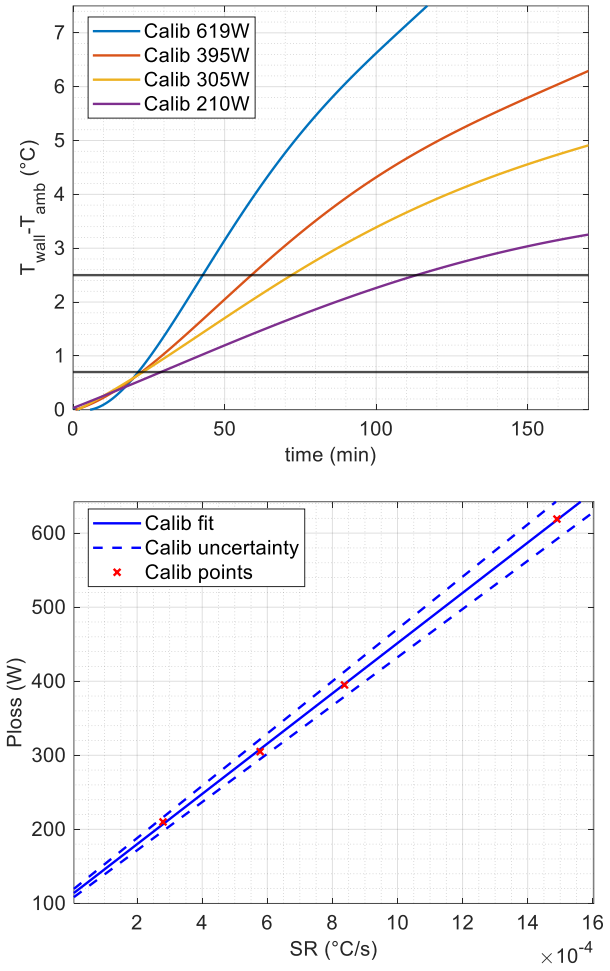

Fig. 9 Top: transient increase of the temperature difference between the tank wall and the ambient (black lines represent the 0.7-2.5 °C ΔT range over which the SR are calculated); bottom: calibration curve of the tank from resistive heating (low SR values are not represented as no measurements are done in this range)

The obtained measured efficiency of the tank is plotted in Fig. 10, along with theoretical calculations from the design phase. A good fit is observed between the measured curve and the theoretical curve at 25°C, with a peak efficiency of the converter tank is measured at 99.16 ±0.04%.

The red curve in Fig.10 corresponds to the losses estimated with the target design of the MFT and the blue curve corresponds to the MFT which was actually manufactured. Indeed, several changes have been made at manufacturing, after the design. In particular, the magnetic core material used in transformer implementation (Ferroxcube 3C90) differs from the original design (TDK N87). The used material has higher core losses, and with higher dependence on the core temperature.

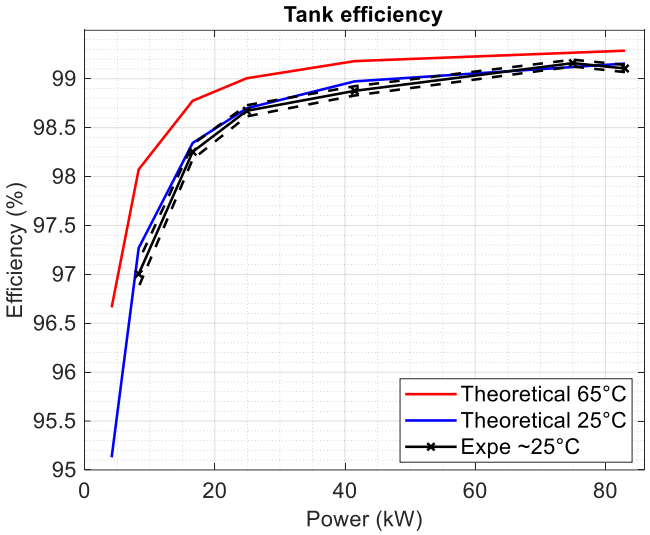

Fig. 10 Measured and theoretical efficiencies of the tank (the efficiency of the LV inverter is not presented here).

This last point is particularly important as the experimental measurements are performed with the transient calorimetric method starting at ambient temperature. Thus, the blue curve is represented for 25°C operation, instead of the anticipated steady-state temperature of 65°C, in order to be compared to the measured values.

5 Discussion on the pros and cons of the method

The pros of the in-air transient calorimetric method can be summarised as:

- Precision compared to electrical methods (here uncertainty < ±0.13 percentage points, ±0.04 at full power; compared to ±0.83 with electrical method [9])
- Rapidity compared to steady-state calorimetric methods (here ~2 h for the lowest power point, ~20 min for the highest power; compared to ~1 day per point for steady-state)
- Ease of implementation compared to transient adiabatic methods in liquid (no stirring needed; no thermal insulation required to ensure adiabaticity)

However, as the power losses are dependant of the temperature and measurement is done during the temperature transient, the measured losses do not correspond to the steady state losses of the converter. A lower operating temperature has a decreasing effect on the losses in the diodes and the MFT copper losses but an increasing effect on its core losses. Hence the different losses at the low power operating points of the converter will tend to be overestimated or underestimated at the high-power operating points. This effect of the temperature on the power losses also brings a trade-off in the choice of the temperature range over which the SR is calculated.

Having a wide range of temperature over which the SR is calculated enables to have a low uncertainty on the temperature difference measurement but makes the measurement phase stray from the calibration phase, bringing errors in the power losses estimation.

6 Conclusion

In this paper, an in-air transient calorimetric method originally presented for the measurement of power losses of semiconductor modules in an automotive inverter has been adapted to the measurement of the losses inside a medium voltage oil tank. This paper has shown that by using calibration resistors, a robust calibration graph can be obtained. The use of a temperature measurement on the wall of the tank has been shown to be more robust (compared to in oil) to variations in the position, orientation, and nature of the actual losses source. The application of the measurement method to a full-scale medium voltage prototype yielded results close to theoretical values. The tank maximum efficiency has been measured at 99.16 ±0.04% (99.12…99.20%).

Acknowledgments

This work was supported by a grant overseen by the French National Research Agency as part of the “Investissements d’Avenir” Program (ANE-ITE-002-01).

The authors also thank Ms. Marion Bonnay for her support in the tests realised during her internship.

7 Appendix

The calculation of uncertainties for the calibration curves is based on the work presented in [14]. For each calibration point, the uncertainties come from the tolerance of the instrumentation used to measure temperature and the injected power. The respective tolerances of the PT100 temperature sensor, and the power analyser considered here are given below:

$$U(S_r) = 0.05\ °C/s \tag{3}$$

$$U(P_{dc}) = 0.01\ W \tag{4}$$

The calibration curve for power losses is an affine function with coefficients A and B such that:

$$P_{loss}(S_r) = A\ S_{r,measured} + B \tag{5}$$

Considering points $(S_{r,1};\ P_{dc,1})$ and $(S_{r,2};\ P_{dc,2})$, it is obtained the following relationships for the slope coefficient A, and the offset B:

$$\frac{\mathrm{U(A)}}{A} = \sqrt{\begin{matrix}\left(\frac{U(P_{dc,1})}{P_{dc,2} - P_{dc,1}}\right)^2 + \left(\frac{U(P_{dc,2})}{P_{dc,2} - P_{dc,1}}\right)^2 \\ + \left(\frac{U(S_{r,1})}{S_{r,2} - S_{r,1}}\right)^2 + \left(\frac{U(S_{r,2})}{S_{r,2} - S_{r,1}}\right)^2\end{matrix}} \tag{6}$$

$$\frac{\mathrm{U(B)}}{B} = \sqrt{\begin{matrix}\frac{\left(S_{r,2}\ U(P_{dc,1})\right)^2 + \left(S_{r,1}\ U(P_{dc,2})\right)^2}{(P_{dc,2}\ S_{r,1} - P_{dc,1}\ S_{r,2})^2} \\ + \frac{(P_{dc,2} - P_{dc,1})^2\ (\left(S_{r,2}\ U(S_{r,1})\right)^2 + \left(S_{r,1}\ U(S_{r,2})\right)^2)}{(S_{r,2} - S_{r,1})^2\ (P_{dc,2}\ S_{r,1} - P_{dc,1}\ S_{r,2})^2}\end{matrix}} \tag{7}$$

To assess the uncertainty in the estimated value of P_{loss}, the error propagation formula, where the a_i are the errors which affect P_{loss}:

$$U(P_{loss}) = \sqrt{\sum_{i=1}^{n} \left(\frac{\partial P_{loss}}{\partial a_i} \cdot U(a_i)\right)^2} \tag{8}$$

This gives the following uncertainty for the P_{loss} value estimated for a given efficiency measurement:

$$\begin{aligned} &U\left(P_{loss,estimated}\right) \\ &= \sqrt{\left(A\ U(S_r)\right)^2 + (S_r\ U(A)^2 + \left(U(B)\right)^2} \end{aligned} \tag{9}$$

References

[1] F. M. Alhuwaishel, A. K. Allehyani, S. A. S. Al-Obaidi, and P. N. Enjeti, 'A Medium-Voltage DC-Collection Grid for Large-Scale PV Power Plants With Interleaved Modular Multilevel Converter', *IEEE Journal of Emerging and Selected Topics in Power Electronics*, vol. 8, no. 4, pp. 3434–3443, Dec. 2020.

[2] H. A. B. Siddique, S. M. Ali, and R. W. De Doncker, 'DC collector grid configurations for large photovoltaic parks', in *2013 15th European Conference on Power Electronics and Applications (EPE)*, 2013, pp. 1–10.

[3] P. Le Métayer *et al.*, 'Break-even distance for MVDC electricity networks according to power loss criteria', in *2021 23rd European Conference on Power Electronics and Applications (EPE'21 ECCE Europe)*, 2021, pp. 1–9.

[4] 'CNR innove dans les énergies renouvelables en lançant son 1er démonstrateur de parc photovoltaïque grand linéaire bifacial vertical', *CNR*. [Online]. Available: https://www.cnr.tm.fr/actualites/cnr-innove-dans-les-energies-renouvelables-en-lancant-son-1er-demonstrateur-de-parc-photovoltaique-grand-lineaire-bifacial-vertical/. [Accessed: 14-Dec-2022].

[5] M. N. Ngo *et al.*, 'Implementation and Characterization of a 200-kW Full-SiC Isolated DC/DC Converter for Future Medium Voltage PV Plants', in *PCIM Europe 2023; International Exhibition and Conference for Power Electronics, Intelligent Motion, Renewable Energy and Energy Management*, 2023, pp. 1–9.

[6] P. Le Métayer, Q. Loeuillet, F. Wallart, C. Buttay, D. Dujic, and P. Dworakowski, 'Phase-Shifted Full Bridge DC-DC Converter for Photovoltaic MVDC Power Collection Networks', *IEEE Access*, 2023.

[7] P. Dworakowski, P. Le Métayer, C. Buttay, and D. Dujic, 'Unidirectional step-up isolated DC-DC converter for MVDC electrical networks', presented at the CIGRE Session 2022, 2022.

[8] P. Le Metayer, H. Reynes, P. Dworakowski, C. Buttay, and D. Dujic, 'Design of Oil Insulated SiC Diode Rectifier for an MVDC SST', in *PCIM Europe 2023; International Exhibition and Conference for Power Electronics, Intelligent Motion, Renewable Energy and Energy Management*, 2023, pp. 1–9.

[9] D. Rothmund, T. Guillod, D. Bortis, and J. W. Kolar, '99.1% Efficient 10 kV SiC-Based Medium-Voltage ZVS Bidirectional Single-Phase PFC AC/DC Stage', *IEEE J. Emerg. Sel. Topics Power Electron.*, vol. 7, no. 2, pp. 779–797, Jun. 2019.

[10] H. Akagi, T. Yamagishi, N. M. L. Tan, S. Kinouchi, Y. Miyazaki, and M. Koyama, 'Power-loss breakdown of a 750-V, 100-kW, 20-kHz bidirectional isolated DC-DC converter using SiC-MOSFET/SBD dual modules', in *2014 International Power Electronics Conference (IPEC-Hiroshima 2014 - ECCE ASIA)*, 2014, pp. 750–757.

[11] F. Forest *et al.*, ‘Use of opposition method in the test of high-power electronic converters’, *IEEE Trans. Ind. Electron.*, vol. 53, no. 2, pp. 530–541, Apr. 2006.
[12] D. Christen, U. Badstuebner, J. Biela, and J. W. Kolar, ‘Calorimetric Power Loss Measurement for Highly Efficient Converters’, in *The 2010 International Power Electronics Conference - ECCE ASIA -*, Sapporo, Japan, 2010, pp. 1438–1445.
[13] N. Mary, R. Perrin, S. Mollov, and C. Buttay, ‘Simple and Precise Calorimetry Method for Evaluation of Losses in Power Electronic Converters’.
[14] A. P. Pai, T. Reiter, O. Vodyakho, I. Yoo, and M. Maerz, ‘A calorimetrie method for measuring power losses in power semiconductor modules’, in *2017 19th European Conference on Power Electronics and Applications (EPE’17 ECCE Europe)*, 2017, p. P.1-P.10.
[15] P. Le Métayer, ‘Unidirectional high-ratio DC-DC converter for renewable energy sources’, Doctoral thesis, INSA Lyon, 2024.
[16] C. Mathieu de Vienne, ‘Étude et réalisation d’interrupteurs haute-tension par mise en série de MOSFETs SiC pour contribuer au développement des applications de transport électrique en MVDC.’, Doctoral thesis, Université Grenoble Alpes, 2023.